Leo Sold

Fieldwork report AG-212
Holocene and Modern Climate Change in the High Arctic
University Centre in Svalbard

Snowmelt 2008 in Linnédalen

Leo Sold
Geography, Mathematics (Staatsexamen LA)
Eberhard Karls University Tübingen, Germany
Phone: +49 (0) 7071 1462041
Email: leosold@yahoo.de

UNIS

EBERHARD KARLS
UNIVERSITÄT
TÜBINGEN

Contents

1 Introduction

The Linnédal is situated on western Spitsbergen, on the southern side of the Isfjord inlet. On an elevation close to sea level, the valley is oriented almost in south-north direction. Linnébreen marks its south end and feeds a river-lake system consisting of Linnéelva and Linnévatnet. The lake is situated at the north end of the valley and its sediments form a basis for the *Svalbard REU program's* research. This project is to contribute to a better understanding of how environmental changes affect fluvial systems and therewith sedimentation, particularly in Linnédalen.

Snow is the most common form of precipitation in northern ecosystems and a large part of the annual precipitation is stored in this solid state during winter and then released as runoff in spring within only a couple of days. This leads to peak river discharge and water levels and can contribute to melting of river and lake ice. (Pohl & Marsh, 2006: 1776)
Furthermore, the duration of absent snowcover during summer marks the time of thawing the upper parts of the in situ permafrost, the active layer. This makes the soil susceptible to transportation and denudation. Therefore, understanding the melting process is important to get a fine grasp of transportation and sedimentation in the hydrological system Linnédalen.

Apart from the discharge and sedimentation effects in Linnédalen, the presence of snowcover is also interesting on a larger scale. It acts a part in present climate change research as it is done for the IPCC Assessment Reports:

> *"Snow, ice and vegetation play vital roles in the global climate system, through albedo and insulation effects. Since the [IPCC Third Assessment Report in 2001], increasing evidence has emerged indicating a more rapid disappearance of snow and sea-ice cover in some areas […], and consequent changes of albedo may be leading to further climate change […]."*
> (Anisimov et al, 2007: 661)

This project focuses on the snowmelt process in Linnédalen to establish a better understanding of hydrologic matters taking place in this mesoscale area. Since the fieldwork was part of the UNIS AG-212 course in summer 2008, the spring melt

2008 was exemplary chosen for analysis.
There is no data about the actual snow depth in Linnédalen available, so data had to be achieved using a different way. This is done by analysing pictures of a time-lapse camera with adequate software to gain data about snow-covered area (SCA). The snowcover data is compared with weather information as well as information from temperature and radiation sensors within the snowpack. For calibration, additional data about the snowpack was taken in the field. The outcome is a detailed image of the spring-melt 2008 that can help to understand when and how the melting takes place.

2 Background

2.1 Phases of the melt period

The melt period starts when the snowpack's net energy input is constant positive (Dingman, 2002: 185). From the hydrological aspect, this period can be separated into three phases, which will be used to structure the analysis part:

- The **warming phase**: Before any melting of the snowpack can occur, its temperature has to be on the melting-point of 0°C. The cold content, the lack of energy that is necessary to warm up the snowpack until it is isothermal on 0°C, has to be 'removed'. The warming phase does not necessarily start with air temperatures above 0°C, but at the point where temperatures within the snowpack start to increase.
- The **ripening phase**: Analogous to the field capacity of soil, snow can retain a certain amount of water in pore spaces between snow grains. As soon as melting occurs, pores start to get filled with meltwater, which is kept in the snowpack by surface-tension forces.
- The **output phase**: When the holding-capacity for liquid water is reached ("ripe"), the snowpack cannot retain more meltwater in the pore spaces. Any further energy input now produces water output. (Dingman, 2002: 185-190)

2.2 Factors contributing to snowmelt

Modelling snowmelt

Today's research offers a couple of ways how to model snowmelt. They are based on different approaches of how to estimate the energy available for melting and vary a lot in accuracy but also complexity. The idea of this work is not to model snowmelt, but to get an idea about which factors contribute to melting. Snowmelt models require quantification of these factors and are therefore brought up here.

The **Temperature-Index Approach** is based on air temperature data and assumes that daily snowmelt (in mm/day) is a linear function of temperature. This kind of models need to be calibrated by a "degree-day-factor", the assumed amount of melting per day per degree (mm/°C day), and a temperature-threshold that is usually around 0°C. This approach can give a good estimation of daily snowmelt if the degree-day-factor suits the local conditions. (Dingman, 2002: 210)
Gray and Male (1981: 418) provide a way to calculate this degree-day-factor. Their formula is based on

- Snow albedo, changing with time
- Vegetation canopy density (can be neglected here)
- Solar radiation: index of actually received solar radiation, reduced by slope and aspect

The **Energy-Balance Approach** tries to actually quantify the energy fluxes on the snow surface with the assumption that all energy is used for melting when the surface temperature exceeds 0°C. The energy balance can be expressed as

$$Q_N + Q_H + Q_L + Q_G + Q_R + Q_M = 0,$$

where Q_N is net radiation, Q_H sensible heat flux, Q_L latent heat flux, Q_G ground heat flux, Q_R is sensible heat flux by rain and Q_M is energy used for melting. Sensible and latent heat fluxes represent the turbulent heat fluxes. A positive sign means a positive energy flux towards the snow surface. The energy available for melting can then be calculated using the latent heat of fusion of snow. (Hock, 2005: 366)
Models using this physical approach require a large amount of data and are fairly complex. They are more sophisticated than the temperature-index models but provide precise snowmelt simulations (Dingman, 2002: 210, 212).

The two main approaches can be combined to obtain a **Hybrid Approach**, an advanced version of the Temperature-Index, to improve the accuracy by including variables that characterise solar radiation properties. It requires less data than the energy-balance and still gives good results. (Dingman, 2002: 211-214)

For this work this means that temperature alone cannot be taken as *the* proxy for melting. More factors need to be taken into account. The degree-day-factor in the Temperature-Index Approach already shows that radiation plays a major role for the energy budget of a snowpack. Taking a closer look to the energy balance formula helps to make out major contributing factors.
In the energy balance formula Q_N is referred to as the net (all-wave) radiation. According to Hock (2005: 368f) it can be written more precisely:

$$Q_N = \underbrace{(I + D_s + D_t)}_{\text{global radiation}}(1-\alpha) + L_s^{\downarrow} + L_t^{\downarrow} + L^{\uparrow}$$

where on the shortwave side I is direct solar radiation, D_s is diffuse sky radiation and D_t is reflected radiation from surrounding terrain. A part of it gets reflected from the surface, represented by the albedo α. On the longwave side L_s is radiation from sky, L_t from surrounding terrain and L the emitted longwave radiation.

Shortwave radiation

The energy input from shortwave radiation is basically dependent on geographical location, season and time. The division into direct (I) and diffuse (D) components is done because parts of the solar radiation are reflected and scattered by clouds and aerosols. In mountainous regions reflected shortwave radiation from the surrounding terrain has to be taken into account. (King et al., 2008: 74)
Major influences to the amount of incoming shortwave radiation are therefore the presence of daylight, slope and aspect, the adjacent terrain and the presence of clouds. The terrain affects shortwave radiation not only by providing reflected radiation, but also by reducing direct sky radiation (Hock, 2005: 369f). Clouds interact similarly; they reduce direct solar radiation but increase the diffuse part. Both, terrain and clouds can produce multiple reflections. (King et al., 2008: 74)

Snow **albedo** is studied extensively since it has a large effect on surface radiation properties. Albedo is referred to as the ratio of reflected shortwave radiation to

incoming global radiation on a surface. Hence it directly controls the available shortwave energy input to this surface. The optical properties of snow vary a lot depending on snow wetness, impurities, grain size and properties, the surface roughness and also the properties of the incoming radiation. (Gray and Prowse, 1993: 71f)
Gerland et al. (1999: 2340) point out that the shortwave reflectance of snow is mainly dependent on grain size within the upper 20 cm of the snowpack and the amount of impurities (mostly soot) on the surface. Values vary from 0,95 for clean, fresh snow in early spring to 0,6 for fairly old snow in late spring. Thin or contaminated snowcovers as well as the bare ground show significantly lower values.
The changes in grain size and liquid water content due to snow metamorphism and melting in spring lead to an albedo decrease. Macroscopically invisible and visible particles may successively cover the snow surface and contribute to this effect. Thinning of the snowpack also decreases albedo when reaching a certain value of snow depth because the ground gets "visible" from above. (Gerland et al., 1999: 2341; Winther et al., 1999: 2036f)
Various values for this threshold are published; Gerland et al. (1999: 2341) suggest 20cm. They assume that the albedo decrease together with meteorological values such as precipitation and clouds make up the major part of snow depth decrease when the snowpack is fairly thin. When studying the optical properties of snow at their site near Ny-Ålesung, Gerland et al. (1999: 2341) expected the change of albedo values due to different sun angles to be less than 5% and the albedo increase due to clouds to be fairly small.

Longwave radiation

Snow is fairly sensitive to longwave radiation since it has a very low reflectance for this spectral region. With an emissivity ranging from about 0,99 to 0,98, it acts as an almost perfect black body (Hock, 2005: 366).
The incoming longwave radiation is emitted from the surrounding terrain and particles in the atmosphere, mostly water vapour, carbon dioxide and ozone. The part originating in the atmosphere is therefore highly dependent on cloudiness and amount and temperature of the water vapour (Hock, 2005: 372). Furthermore, due to the strong absorption by water vapour, it is mainly determined by the conditions within the lowest few hundred meters in the atmosphere (e.g. King et al., 2008: 75). This

makes clouds with their high emissivity an important source for energy at the snow surface.
The surrounding terrain affects the longwave radiation on the one side by obstructing the sky and decreasing incoming radiation (like for the shortwave radiation) and on the other side by emitting additional radiation itself (Hock, 1999: 374).

The **effect of clouds** on the surface energy balance is opposite for long- and shortwave radiation. King et al. (2008: 76) point out that on snow with its high albedo, the loss of shortwave radiation due to cloud cover usually is less than the increase in longwave radiation. In polar regions, were sun angles are low and cloud transmissities and albedo are high, this situation of increased energy input due to clouds is most likely to occur.
The same is identified by Zhang et al. (1996: 2121) as they show that thin and low clouds have a more positive effect on the snow surface energy balance as high and thick clouds. Additionally, they conclude that the effect of clouds on snowmelt is generally high in the beginning and decreases as the season progresses. The onset of snowmelt occurs significantly earlier under overcast than it does under clear sky conditions. (Zhang et al., 1996: 2121)

Turbulent heat fluxes

The turbulent heat fluxes, referring to Q_H, Q_L and Q_H in the energy balance formula, represent another source of energy to the snow surface. The fact that snowmelt is dependent on air temperature indicates the importance of turbulent heat transfers. Both, latent and sensible heat fluxes, increase with wind speed above the surface and the difference between the air and the surface regarding the respective value – temperature for sensible heat and vapour pressure for latent heat. (Gray and Prowse, 1993: 21)
Rain falling on snow with a temperature below the freezing point will first release sensible heat until it reaches the freezing point. Then the water freezes, releasing latent heat. If the snowpack is isothermal at freezing point, the water will only release its sensible heat, which is then available for melting. (Dingman, 2002: 199f; Gray and Prowse, 1993: 22)
In both cases, rain means a positive energy flux towards the snow surface and contributes either to the warming or the melting of the snowpack, because snow does not exist with temperatures above the freezing point. When the rain does not freeze

the latent heat of fusion is not released, making rain more effective for warming than for melting.
In regions where the snowcover develops patchy patterns during the season, the **local scale advection** can significantly contribute to the point energy budget on the snow surface. Snowpatches and snow-free areas show large differences in surface physics that arise in surface temperature and albedo. Local advection of sensible heat from the snow-free areas to the snowpatches can provide additional energy and increases with decreasing SCA (and patch size) as it is shown in ‣ Figure 1. (Marsh, 1999: 2124f)

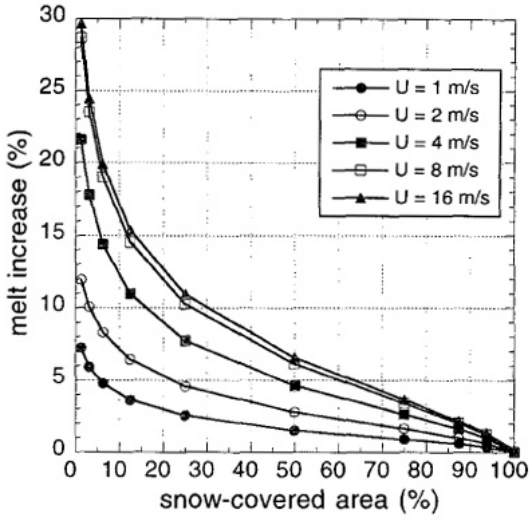

Figure 1: melt increase due to local scale advection of sensible heat. Source: Liston (1995 p1711)

According to e.g. Gray and Male (1981: 395), the **ground heat flux** can be safely neglected for short-term periods. Compared to other energy fluxes it makes up an insignificant part in the energy balance.

3 The Plumecam

"The Plumecam" is an automated digital camera that is placed on the eastern side of Linnévatnet near to its south end. The camera is a Pentax K110D that sits in a protecting case behind a glassed opening. It is solar powered and takes 2 images a day – ca. 11:00 and 16:00 o'clock (spring 2008) – which are saved in the jpeg file format onto a standard memory stick. The resolution of the images is 3008 x 2000 pixels. The camera was in automatic mode, so that it chose the right exposure time and F-Number for not over- or underexposing the pictures.

Figure 2: Plumecam case with solar panel

The wooden case sits directly on the rocks on a basalt ridge (see ‣ Figure 2). The map (‣ Attachment 6, page 41) shows place and viewing angle of the camera. Its view

covers an approximately triangular shaped area in the Linnédalen. The Linnévatnet takes up a lot of space on the images; as well as the sky and some rocks in the foreground, which are sitting on the basalt ridge. It turned out that in the end only one third of the image caption could be used for the actual analysis. Originally the camera was installed to watch the changing of size, form, position and colour of the plume behind the lake's inlet ("*Plume*cam").

4 Methods

4.1 Plumecam-picture analysis

The basic idea of how to extract data about the snow out of the pictures is to use a "Threshold Filter" in an image editing software. This filter remodels the colours in a picture using a threshold value for brightness. Every pixel that is darker than this certain value is changed to black colour, every brighter pixel to white. Some simple try-outs showed that this is a good option for separating snow from other landscape in the pictures.
After this separation is done, a standard image analysis tool, the "Histogram" is used to count the black and white pixels. Assuming that a black pixel now means land-surface and a white pixel means snow-covered-surface, the ratio of white pixels to total pixels can be interpreted as the *snow-covered area* (SCA) (as a value between 0 and 1). Doing this for a time-series of pictures throughout the spring allows plotting the SCA on a time scale.
Of course, this value has to be handled carefully. Topics like the relation of SCA and snow-water-equivalent or the influence of transformation due to view angle and perspective will be discussed.

The way of analysing the Plumecam pictures can be summarised in a couple of steps that will be described in the following chapters:

1. Select a timeframe that is interesting concerning the spring melt event
2. Prepare the pictures
3. Apply a "Threshold Filter" to all images (‣ Figure 3b)
4. Cut out not-interesting parts (foreground, lake, sky) (‣ Figure 3c)
5. Count black and white pixels in every image

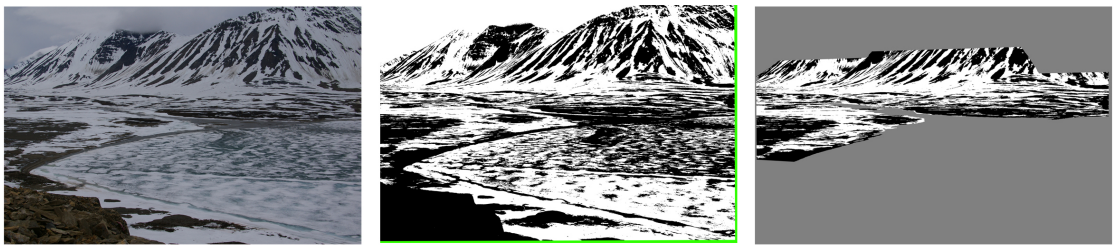

Figure 3: Image analysis stages

Selecting a timeframe

The starting point is the 17.05.2008, which is shortly before there is any change in SCA visible in the pictures. The last analysed picture is the 11.08.2008 when the cameras memory stick was downloaded because the fieldwork ended. However it turned out that this date fits good to the ending of the melting season.
The camera took two pictures a day, on 11am and 4pm. Only the 11am pictures are used for analysis, because of the time difference of only five hours and more shadows on the valley slope on the 4pm-pictures.

Preparing the images

The Plumecam-case sits directly on the ground on the basalt ridge. When it was installed there was no good reason to prevent it from moving slightly, so it wasn't fixed to stable ground. Thus, during the spring water in the ground melted, resulting in surface lowering and some moving of the stones the case was placed on. Since the camera moved a little, the image caption changed a bit. This is not a big deal when the images are used for a qualitative analysis, but in this case some regions will be cut out (lake, sky and foreground) and the results should be as precise as possible.
For all the 87 pictures (or days) respect to this little motion is taken by using standard image editing software for moving and rotating the image to fit the position the camera had on the 13.07.2008.

Applying the Threshold Filter

Image editing software like Adobe Photoshop offers a "Threshold Filter". This filter remodels the colours of the image using the brightness of every single pixel. Darker pixels are changed to black, brighter pixels to white. The brightness-value that

separates ‘dark’ from ‘bright’ can be adjusted between 0 (black) and 255 (white). For many of the pictures 128 (50%, mid grey) does a good job as threshold value. It works fine as long as there is some kind of ‘grey’, cloudy weather. Sunshine makes the whole image brighter and produces some shadows at the same time. The camera responds with a shorter exposure time. In this case the threshold value has to be smaller and it is difficult to find a value that still works in the shadow-parts of the image. The threshold value has to be adjusted for every single image, but the same value can be used under the same weather conditions.

Cropping the “Active Area”

Some regions on the Plumecam’s pictures are not interesting for studying the snowmelt process. Of course, the sky is one of them, but also the parts that are covered with water are not taken into account. The snow on the frozen lake melts under very different conditions and does not even play a role for water runoff. The boulders on the basalt ridge in the foreground are too close to the camera for giving useful results when studying the melting process in the whole valley. Furthermore, the cirque on the picture’s right end is heavily affected by shadows and the higher parts of the valley’s western slopes are frequently covered by clouds. Hence, both are cut out to prevent problems during the analysis. Because the lake’s heat capacity may affect the melting process in some way the small stripe of land between the lake and the image bottom is excluded as well. Due to perspective bias it makes up a large area on the pictures although it is only a couple of meters wide.

The leftover makes up approximately one third of the original image area and can be described as “valley floor and lower parts of the western slopes”. Some image editing software like e.g. Adobe Photoshop offers not only the selection tool but also the possibility to “batch process” a bunch of pictures. This helps saving time because the process (select area and cut it out) can be “recorded” and then be applied to all the 87 pictures at once.

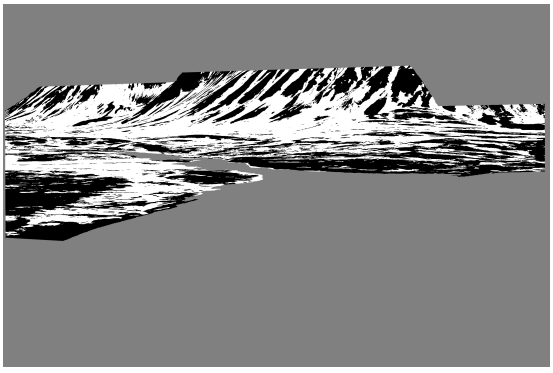

Figure 4: “Active Area” with applied threshold filter on the 27th of June

The cut-out-areas are coloured in mid grey. In the next step this allows to only count pixels in the “Active Area”, which are either black or white. ‣ Figure 4 shows an example for how the “Active Area” looks like in this step of analysis.

Extract the data

So far, the pictures consist of three different colours: The ‘snow’-pixels are white, the ‘landscape’-pixels are black and the parts which are not taken into account are grey. Using the “Histogram” analysis tool now allows telling exactly how many pixels have a certain brightness. ‣ Figure 5 (bottom) shows a histogram during analysis, where the spike in the middle represents the non-active parts that are coloured grey, the zero-spike represents land surface and the 255-spike stands for the snow-covered area. A simple equation now provides the percentage of SCA in the “Active Area”:

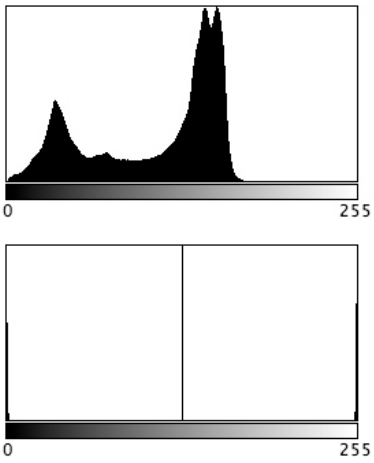

Figure 5: Histogram examples. Top: original image 26th of June. Bottom: same image during analysis.

$$SCA = \frac{P_{white}}{P_{white} + P_{black}}$$

with P_{white} as the number of white pixels
and P_{black} as the number of black pixels

The “Active Area” is split into three regions that can be analysed separately separately:

1. The valley’s western slopes (‣ Figure 6a)
2. Western valley floor (‣ Figure 6b)
3. Eastern valley floor (‣ Figure 6c)

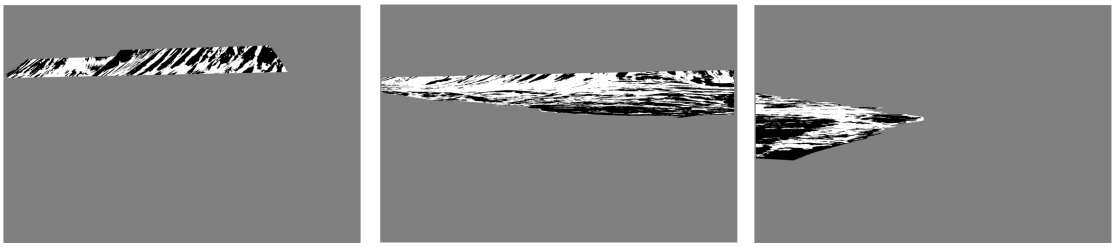

Figure 6: Splitting of the "Active Area"

It is interesting to study these regions separately because the snow distribution also depends on the topography; wind drift plays a big role and the main wind direction is west. Additionally, these regions are differently exposed to the camera. The western slopes are tilted and therefore more exposed than the valley floor on the western side. The eastern valley floor is closer to the camera than the western one. This has to be taken into account as otherwise the foreground is weighted higher in the results.
It will be discussed later whether this is a proper way of respecting the perspective bias.

The Outcome

For every picture in the time series the outcome of this method is:

Timestamp	SCA: "Active Area"	SCA: western valley slope	SCA: western valley floor	SCA: eastern valley floor

This works nicely for plotting and offers a clearly arranged way of "watching the snow melt" during the spring.

4.2 Measuring a snowpatch

The picture-analysis tool has to be calibrated in some way; otherwise its SCA-data doesn't help to understand the melting process, which actually means the decreasing of the snow's water equivalent. The fieldwork at Kapp Linné allowed arranging a set of measurements on the snowpack. At this point the main part of the melting event was unfortunately already over.

The measurements were performed on a snowpatch on the western valley slope, which is well exposed to the Plumecam. This allows comparing the results of both methods later on. The position is marked on the map (‣ Attachment 6, page 41).
The measurements that are set up as a time series were performed every other day between the 24/26.7.2008 and the 9.8.2008.

Exposure

The exposure of the snowpatch was documented based on two different aspects. The direction of exposure and inclination was taken using a handheld compass with built-in inclinometer. Because of the mountainous landscape and its position on the valley

slope, the solar shading of the snowpatch ("effective horizon") was documented as well. Starting in the north, every 30 degrees the angle between the horizon and the uppermost point of landscape in this direction was measured.

The radiation is one of the major energy sources for the melting process and varies a lot with effective horizon, aspect and inclination. The solar shading by the surrounding terrain reduces the incoming shortwave radiation as sunlight and as diffuse radiation from the sky. Furthermore, the terrain plays a role for the longwave radiation coming from the atmosphere but also from the surrounding landscape. (Hock, 2005: 366, 368)

Snowpatch size

The snowpatch's shape can be described as "approximately right-angled triangular" (› Figure 7). It kept its shape while melting during the period of measurements that were done every other day. It is not sure whether it outlived the summer or even several years. For getting an approximate value for real SCA the side lengths of the triangle were measured using a large-scale tape measure. The maximum extend of the snowpatch in up-slope, northern and southern direction was taken as corners of a right-angled triangle to approximate the size.

Figure 7: The gauged snowpatch on the 24th of July

Snow density and water equivalent

The snow water equivalent (SWE) is the actual amount of water stored in a snowpack. It is expressed as vertical depth of the water layer if the snow would be melted and is measured in millimetres like liquid precipitation (Armstrong & Brun, 2008: 187).

A density measurement and the snow depth are necessary to calculate the SWE:

$$SWE(mm) = \rho\left(\frac{kg}{m^3}\right) \cdot d(m)$$

with ρ as the snow density
and d as the snow depth
(Armstrong & Brun, 2008: 187).

The density was taken using the gravimetric method for the whole snowpack at once. This eliminates information about the layering of the snowpack but it provides a correct mean value. A vertical column of the snowpack with a known volume is weighted. The standard unit is kg/m^3. (Armstrong & Brun, 2008: 187)

Snow depth

The snow depth can be measured easily without a lot of effort. The American Avalanche Organisation (2004: 14) suggests choosing a white stake when left in the snowpack to reduce melting caused by the stake's radiation properties. The snow around the stake should stay as undisturbed as possible. The depth is not measured orthogonal to the snow surface but vertically. (American Avalanche Association, 2004: 14)

On the snowpatch in Linnédalen the snow depth was measured every other day using two different setups. In the centre of the triangular shaped patch the depth was always checked and averaged at the same five points. The points were spread within approximately 0,5m^2 and the stake was removed after gauging to avoid radiation from it.
In addition, the depth was checked along a stretch at the lower part of the patch. Values were taken every meter on both sides, an arm-length away from always the same stretch. ‣ Figure 8 shows the gauging locations on the patch.

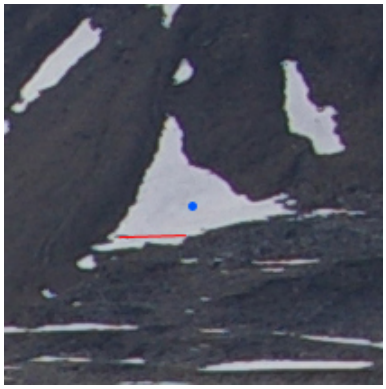

Figure 8: Location of measurements. Blue dot: snow depth stakes. Red line: depth stretch

4.3 The Snowtree

The “Snowtree” is deployed on the eastern side of Linnéelva, just beside the river, approximately on half way between Linnévatnet and Linnébreen. It is a 45cm stake, vertically fixed in the ground. On 7, 15, 30 and 45cm above the ground it has horizontal ‘branches’ (“tree”) with Hoboware sensors on them, measuring brightness (horizontally directed) and temperature every 30 minutes. With increasing snow depth, more sensors get buried, the brightness measured by these sensors decreases and they provide information about temperatures within the snowpack.

4.4 Weather station data

A Hoboware weather station on the valley floor, near the south end of the lake (position marked on the map: ‣ Attachment 6, page 41), provides numerous weather data for the valley. This data will be related to the SCA-data from the Plumecam-pictures.
On a 30 min resolution it measures the following weather elements:

- Air temperature (°C)
- Soil temperature (°C) in 0,5m and 1m depth
- Liquid precipitation (mm)
- Wind speed (m/s) and direction
- Air pressure (Hg)
- Solar radiation (W/m2) up- and down-looking

Unfortunately the humidity sensor did not work during the period of measurements. The liquid precipitation values have to be handled with care because snowfall measurements in such gauges are highly affected by wind (Dingman, 2002: 169f) and meltwater in the gauge produces positive precipitation-data.

Furthermore, a simple temperature logger is situated on the Little Ace Age moraine of the cirque on the slope of Griegfjellet, just southwest from the lake’s southern end. It is placed under a radiation shield and measures temperature and air humidity on a 30-minute scale. It is taken into account in addition to the main weather station because it is situated closer to the snowpatch that was gauged under comparable exposure properties.

5 Results

5.1 Plumecam-picture analysis

The Plumecam's pictures were analysed starting with the first picture on the 17.05.2008 up to the 11.08.2008 – fitting the first visible changes in SCA in the beginning and the last changes as well as the fieldwork in the end.

The slight moving of the ground, which affected the image caption by moving the camera case a little, happened approximately between the 15.06.2008 and the 13.07.2008. The foreground in the bottom left of the pictures shows the stones creeping. This happens before the camera case actually moves: between the 26.05.2008 and 10.06.2008.

Because of bad weather conditions or water drops on the glassed opening of the case, 18 of the 87 pictures were dropped. Their dates are listed below.

- 29.05.2008 (low clouds)
- 30.05.2008 (low clouds)
- 31.05.2008 (low clouds)
- 01.06.2008 (very low clouds / fog)
- 02.06.2008 (water drops on glass)
- 22.06.2008 (clouds & water drops)
- 04.07.2008 (very low clouds)
- 05.07.2008 (low clouds)
- 09.07.2008 (low clouds)
- 11.07.2008 (water drops)
- 12.07.2008 (water drops & clouds)
- 19.07.2008 (water drops)
- 21.07.2008 (water drops)
- 27.07.2008 (low clouds)
- 01.08.2008 (low clouds)
- 02.08.2008 (low clouds)
- 03.08.2008 (fog / low clouds)
- 04.08.2008 (low clouds)

The data is attached in combination with the weather data as a full-page table (‣ Attachment 1, page 36). A plot is included as ‣ Attachment 5, page 40.

5.2 Weather station data

Due to the 30-minutes resolution of the sensors, the dataset from the weather station was fairly bulky and the data had to be aggregated. It is contained in the main result table (‣ Attachment 1, page 36), scaled down to daily values. The following measurements are taken into account:

- Precipitation (summed up for each day)
- Temperature (daily average)

- Wind speed (daily average)
- "Albedo" (Calculated as the daily average of the ratio of down- to up-looking radiation sensor values)

The daily average of temperature is calculated by taking the real average from all values per day. No values were weighted more than others in the calculation as it is done for some other purposes.

5.3 Snowtree

The snowtree data consists of temperature and radiation values on a 30-minutes-scale. The values in the table are scaled down to daily averages. The radiation values are not taken into account, since they cannot provide albedo data (directed horizontally). Additionally, precise information about when snow depth decreases down to certain values is not useful with such a coarse graduation (7cm, 15cm and 30cm). The sensor 45cm above ground broke off his branch at an unknown point during the winter and is therefore not listed in the results.
The noticeable 'stepwise' temperature increase originates in the graduated sensibility of the Hoboware sensor. This is obvious in the raw data.
The dataset can be found as ‣ Attachment 3 on page 38.

5.4 Snowpatch on the western slope

Exposure and effective horizon

The exposure data including aspect, inclination and effective horizon was taken on the 28.07.2008 using a Recta DS 50G handheld compass for both, direction and inclination. The elevation was measured with an altimeter, calibrated at Linnévatnet, to avoid major barometric effects due to weather changes.

- Aspect: ENE
- Elevation: 117,75masl
- Inclination: 28°

Aspect (°)	0	30	60	90	120	150	180	210	240	270	300	330
Angle (°)	6	7	8	2	6	10	22	30	32	22	16	0

Table 1: effective horizon of the snowpatch on the western slope

Snowpatch size

The snowpatch's extend was measured every other day, from corner to corner, assuming that its shape is right-angled triangular. The triangle's area is simply calculated with $A = \frac{1}{2} \cdot a \cdot c$. Working on the small scale and especially on the rocky ground it was sometimes difficult to place the maximal extend.
Additionally, the Plumecam pictures are analysed to gain data about the snowpatch's size. This works well although it is placed on the other side of the valley since the patch is exposed to the camera due to inclination. The data shows that the values of the picture analysis and the triangle estimation show fairly similar values, at least in the beginning when the patch made up a nice triangle. This indicates that the resolution of the camera pictures is approximately $1m^2$ on the western slope.

Date	Side a (m)	Side b (m)	Side c (m)	Triangle area (m^2)
24.07.08	87,5	56,3	61,4	2686,25
26.07.08	82,1	52,25	56	2298,8
28.07.08	75,8	51,5	54,5	2065,55
30.07.08	56,7	51,5	49,8	1411,83
01.08.08	56	51,2	50,7	1419,6
03.08.08	56,6	51,6	49,4	1398,02
05.08.08	55,6	50,1	47,2	1312,16
07.08.08	54,1	50	47,2	1276,76
09.08.08	53,8	49,6	46,2	1242,78

Table 2: Snowpatch size measurements

Snow density and water equivalent

The density was sampled on the 28.07.2008. A core tube was pushed vertically through the whole snowpack near the centre of the snowpatch. The snow surface was marked on the tube to calculate the volume that the (uncompressed) snow inside the tube had. The snow was weighted with a good kitchen scale and the result got compared with the volume in a scaled cylinder after melting (room temperature) to check the result.

Tube fill length	Tube radius	Snow volume	Snow weight	Snow density
123,5cm	3,3cm	4225,175 cm3	1661g	393,120 kg/m3

Table 3: Gauging snow density

The density information can be used to calculate the SWE, i.e. at the point were the density was measured, by using the 'tube fill length' that equals the snow depth in this case:

Snow depth	Snow Density	SWE
1,235 m	393,120 kg/m^3	485,503 mm

Table 4: Snow water equivalent

Snow depth

The first setup consisting of 5 gauges every other day was averaged and gives a clear data set about the snow depth in the patch's centre. Due to methodical changes after the first time measurements the time series was restarted. Hence it starts two days after the other depth and the size measurements.

Date	Stake 1 (cm)	Stake 2 (cm)	Stake 3 (cm)	Stake 4 (cm)	Stake 5 (cm)	Average (cm)
26.07.08	202	210	210	220	220	212,4
28.07.08	209	205	195	170	196	195
30.07.08	197	160	182	176	189	180,8
01.08.08	188	154	173	168	183	173,2
03.08.08	183	145	163	156	182	165,8
05.08.08	171	136	150	142	171	154
07.08.08	160	128	143	135	158	144,8
09.08.08	153	119	135	132	149	137,6

Table 5: Snowpatch snow depth - stake method

The second way of gauging snow depth produces a dataset with snow depth values for two times 16 points for every timestamp. In this table the two values for every distance-meter from the starting point were averaged (‣ Attachment 4, page 39).

Little Ace Age moraine temperature logger

For a better comparability with the other measurements of the snowpatch, the temperature data from the western slope was averaged from 12:30 to 12:00. So, the temperature value in the table represents the average of the last 24 hours *before* the Plumecam picture was taken and the field measurements (app.) were done. This accounts for temperature changes e.g. in the afternoon which would otherwise be

counted as if they occurred before the picture was taken in noon. The data is given in the overview table (‣ Attachment 2, page 37).

6 Analysis

The dataset of SCA from 17th of May to 11th of August 2008 shows how the snowcover disappears from the valley floor first with increasing, later with decreasing speed (% per day). This leads to an s-shaped graph when the SCA is plotted over time: ablation does fairly little progress in the period before and after the main melting event. During the main melting event, the major part of the snowcover melts within only a couple of days. The slope-SCA is discussed separately, because it doesn't have that convex-concave graph.

The time series starts on the 17th of May with a SCA of more than 99% on the valley floor. At this point and also for the next couple of days, the weather station has not gauged any significant air temperature above 0°C since mid February. Positive temperature data and maybe-melting earlier in this year is not taken into account in this work.

6.1 The Warming Phase

The temperature data from within the snowpack allows us to tell precisely at which point the snowpack is isothermal, but due to the very low thermal conductivity of snow, it takes a while for the warmth to penetrate from the upper surface of the snowpack to the sensors in the bottom. Hence, the starting point of increasing temperature at the uppermost temperature-logger of the Snowtree does not indicate the beginning of the warming phase. The thermal conductivity increases (non-linear) with increasing snow-density; e.g. app. 0,4 W/m°C for a 400 kg/m^3 density (Langham, 1981: 295ff).
If a snow depth and density value for this certain spot and time would exist, the time it took the energy to penetrate through the snowpack could be estimated.

The Snowtree data shows that the warmth comes from the upper snow surface. It 'reaches' the uppermost sensor first, then the lower ones successively. The approximated starting dates for the respective distances from ground surface are

- 7 cm above ground: 26.5.2008
- 15 cm above ground: 10.5.2008
- 30cm above ground: app. 26.4.2008

These dates are difficult to make out because the temperature increases fairly slowly. The two upper sensors don't show real progress before app. the 20th of May. The dates above mark the dates since that the daily averaged temperature didn't decrease.

The snowpack's isothermal state is reached almost isochronous at the three sensors, on the 31st of May; only the 15 cm sensor took a little longer, to the early 1st of June. This marks the end of the warming phase.

The warming of the snowpack requires energy, namely the specific heat of snow. The precipitation gauge doesn't show any significant values for the respective period. The averaged air temperature doesn't rise above 0°C before the 25th of May, resulting in weak sensible heat fluxes before this date, although higher wind speeds occurred from the 21st to 23rd of May. Since albedo doesn't drop below 0,8 until the 24th, shortwave radiation cannot contribute a lot of energy as well.
This makes longwave radiation the major source of energy available for the warming period before the 25th of May. The Plumecam pictures support this thesis as they show overcast conditions from the 20th of May on, longing for the rest of the warming phase.

From the 25th of May on, daily air temperatures exceed 0°C and albedo drops down to 0,69 on 31st of May. The pictures show fairly overcast conditions and low clouds for the rest of the warming phase indicating that longwave can exceed shortwave radiation energy input. Higher windspeeds on the last two days of the warming phase and air temperatures of 1,58°C and 2,2°C on these days contribute some sensible heat flux. The local advection of sensible heat is insignificant for the whole warming phase, since SCA is still almost outright.

The clouds seem to be heavily contributing to the warming. The beginning of 'real progress' in temperature increase within the snowpack corresponds to the appearance of clouds. Very low clouds or fog in the valley dominate the weather conditions in the last two days of this phase, where temperatures rise rapidly within the snowpack – especially for the uppermost sensor.

This is in line with the outcome of the paper by Zhang et al. (1996: 2121), who studied the effect of cloud cover on snowmelt.

The last days of the warming phase show a flood event in the valley, starting on the 28th of May, lasting about ten days. It is not identifiable from the pictures where the water exactly comes from. It shows up as a streamflow on the eastern valley floor, running towards Linnéelva. On the 31st it increases rapidly in size and then covers the entire lake ice with water. Later, on the 3rd of June it drains into the lake through a hole in the ice.
Since the snowpack is not yet isothermal on the 28th of May, the water cannot be meltwater from snow. The large amount of water may indicate a draining event, possibly from Krongressvatnet. Several options for the water's origin were discussed in the field. Since the valley still is completely snow-covered, the water had to drain through the snowpack. This fills up the snow's pore spaces, reducing the amount of running water on the one hand side, but could also cause a feedback effect on the other side. Assuming that the water's temperature is above the freezing point (wherever it comes from), it could provide sensible heat for warming the snowpack and then liberate latent heat when freezing, like it does when rain falls on cold snow. As soon as the snowpack is isothermal, the water's sensible heat would support melting. However, it is unlikely that the water's temperature is significantly above 0°C and furthermore, the non-isothermal state of the snowpack doesn't support the thesis of a snow-meltwater flood.

6.2 The Ripening Phase

As soon as the snowpack is isothermal, all energy input is consumed by melting snow. In spring 2008, this starts on the 1st of June, but it is hard to tell at which point the snowpack is ripe – the setup of measurements didn't contain instruments for measuring liquid water in snow. Additionally, the water from the flood event covers the channel of Linnéelva, making it hard to tell from the pictures whether runoff from snowmelt occurs or not.
However, the optical properties of the snowpack change with its physical properties. The albedo of snow decreases with increasing liquid water content in the snowpack, because it increases the effective grain size (Winther et al., 1999: 2036). Meltwater from the snow surface percolates down and fills up pore spaces and accordingly the liquid-water-holding capacity of the snowpack. On the 6th of June the snow albedo

drops from 0,71 to 0,54 and then stays fairly constant for three days. Afterwards it continues decreasing.
The precipitation gauge doesn't show values for these days, which could cause a significant change in albedo. I assume that this drop in albedo marks the time where the maximum liquid water storage capacity is reached. The weather conditions change slightly from sunny to overcast, but this should only have slight increasing effects to the albedo (Gerland et al., 1999: 2341) and didn't cause significant changes e.g. when weather conditions change between 19th and 21st of May.
The ripening phase therewith takes place from 1.6.2008 to 6.6.2008.

On the first two days of 'ripening', there is no SCA data available, because bad weather renders the picture analysis impossible. These two days show low clouds, humidity and precipitation with temperatures above 2°C.
The precipitation takes place mainly on the 2nd on June, rapidly affecting the albedo. From the 1st to the 2nd it drops down from 0,62 to 0,54, because of the increased liquid water content. At this point, the snowpack is already warmed up, so the rain doesn't refreeze and liberate latent heat. Because the SCA data is missing for these days, the contribution to snowmelt is insecure but probable.

The weather conditions are sunny on the 3rd of June, providing an SCA of still 99,8% on the eastern valley floor and 97,4% on the western floor. Within the next two days, the value on the western floor decreases to 93,8 whereas it stays fairly constant on the eastern side. However, from the beginning of the ripening phase on, the SCA starts decreasing.
The albedo recovers after the rain event, rising from 0,54 (June, 2nd) back to 0,62 on the 3rd and 0,72 on the 4th of June. This can happen because the amount of liquid water underneath the snow surface decreases as water percolates down when the amount of present water originating from the rain event exceeds the holding capacity of the snowpack.

6.3 The Runoff Phase

Until the 21st of June, the decrease in SCA is only slight, represented by an average loss of app. 0,5% per day only. From the pictures, this period shows fairly variable weather conditions ranging from clear sky to overcast, but no precipitation except an insignificant, hardly measurable value on the 11th of June. Temperatures are relatively

low during this time, ranging from 0,17°C to 2,07°C, causing only weak sensible heat fluxes.
The major change for this period of 15 days arises in the albedo. From the 6th to the 20th of June it decreases from 0,54 to 0,29. At this point the albedo values must be handled with care, since the bare ground also reflects shortwave radiation. Later in the season, when the snow is certainly gone, albedo values vary around 0,15-0,20.
As described above, the snowpack gets transparent to shortwave radiation when melting down to a certain depth, making the ground 'visible' from above. This decreases albedo significantly. Assuming that this is the case here, this means that the weather station is now placed on an almost snow-free patch and the values for albedo are now defective regarding their validity for the whole catchment. In the beginning of the runoff phase, the albedo was 0,54, which is already a fairly low value. Hence, albedo will be taken as "fairly low" from now on.
On the 22nd it performs a little jump to 0,36, which should be caused by changes on the bare ground surface. There is no obvious connection to other available data. Afterwards albedo reaches lowermost values.
The meaning of this period of only slow decrease in SCA will be discussed later since decrease in SCA is not a linear function of decrease in water equivalent.

Then, synchronous with the summer solstice, the main, rapid melt event begins. The weather station registered a rain event with 13,2mm on the 22nd of June, involving three more days of less precipitation. This is accompanied by a temperature jump up to 3,38°C. These weather conditions promote melting as it is shown in the SCA data. Within the next two weeks SCA drops down to 14% on the eastern and 28,3% on the western valley floor. This means an (average) loss of over 60% SCA within only 14 days.
Since the beginning of the runoff phase albedo is low, making the snowpack more sensible to shortwave radiation. The rain event from the 22nd to the 25th of June and some other smaller events on the 30th of June and 3rd of July contribute to this fact. Air temperatures stay fairly high during this period, not falling below 2,8°C and reaching a maximum of 6,1°C. In addition, the effect of local advection of sensible heat starts to take place, since the valley now shows a really patchy pattern of snow distribution. Gray and Prowse (1993: 22f) state that the melt of large snowpatches is mainly controlled by radiation and as they decrease in size, turbulent energy fluxes

become the dominating source of energy for melting. This is likely to be the case from about the 3rd of July on.

The period of rapid melt ends on the 8th of July with an SCA of 7,6% on the eastern and 21,7% on the western valley floor. A relatively large rain and wind event from the 10th to the 13th of July reduces the snowcover on the western floor to 13,42%, but doesn't have significant effects on the eastern side, since this is almost snow-free at this point.
However, this rain event involved some slight snowfall, visible on the slope of Griegfjellet, but with the snowline high enough to be out of range for the slope-area in the picture analysis. On the valley floor the daily averaged temperatures remained above 2,3°C.

The precipitation event is followed by a number of warm days with temperatures up to 10,2°C (23rd of July). The SCA on the western side decreases slowly, reaching values below 5% on the 29th of July for the first time.
As soon as SCA is as low as app. 5%, the SCA dataset shows values jumping up and down between 0,2% and 5%. This shows how the analysis method is sensible to reflections from water surfaces such as small streamflows.
The time of postmelt, as SCA decreases slowly, will be analysed more detailed in a following chapter.

6.4 Differences between the western and eastern valley floor

The temporal decline in SCA shoes the same s-shaped curve for both areas on the valley floor. Also changing weather conditions arise similarly in the SCA datasets of the western and the eastern valley floor. Nonetheless, there are differences in the depletion curve.
In the beginning of the ripening phase, the SCA starts decreasing a little on the western floor while landscape stays completely snow-covered on the eastern side. This takes place only for a couple of days, from the 1st to the 8th of June. On the 25th of June, the eastern floor "overtakes" the western one. The decline happens significantly faster on the eastern side than it does on the western side. From then on the SCA constantly stays lower on the eastern side. This stands for differences in snow distribution and terrain roughness, which deform the correlation of snow depth and SCA. The "Discussion" chapter will take this topic on.

6.5 Snow depletion on the western slope

The SCA data also shows how snowcover decreases on the western slope. In comparison with the data from the valley floor, the slope-SCA decreases close-to-linearly. The plot shows several spikes, which are related to changing weather conditions and therewith changing brightness conditions and adjusted threshold values for the analysis.
The depletion is independent from the contributing factors, which were identified on the valley floor. Even the precipitation events don't arise in the slope data. The decrease in SCA starts on the 17th of May with a value of 99%. At this point the snowpack on the valley floor is not isothermal by far. This must be due to differences in snow distribution, since a much higher energy input on the slope can be ruled out. For instance the analysis of the snowpatch data shows that shortwave radiation is definitely lower on this slope.

The difference in local distribution of snow is studied extensively since it acts a part in modelling snowmelt runoff for hydrologic catchments. Pohl and Marsh (2006: 1775f) point out that arctic environments show high rates in wind redistribution of snow because of their open and exposed landscape and their cold winters without freeze-melt-cycles that stabilize the snowpack. Snow is preferentially scoured from exposed locations as slopes and deposition takes place as wind speed decreases in the lee of topographic features.
In this case this results in a complex pattern of snow distribution where snow depth in average is low on the slope, but gets trapped in cracks and small lee areas where it melts successively.
Because of the small water equivalent on the slope and the independence from weather conditions, the melting on the western slope cannot contribute significant runoff or peak discharge to the hydrologic system in Linnédalen. In this work it is therefore not discussed in further detail.

6.6 Postmelt period on the western slope

Figure 9: Snowpatch size decrease from 26th of July (grey) to 9th of August (white).

The snowpatch on the western valley slope was measured every other day during the phase after the main melt event. The dataset shows a fairly constant decrease in snow depth and size through two weeks. On the 26th of July, when the first complete set of values is available, the patch's size is 2362px; the triangle approximation gives a value of 2299m^2. The snow depth is 212,4cm as the average of the 5 measurements on the snowpatch.
Through the period of 15 days, the snowpatch lost 36% in size, according to the Plumecam-pictures (‣ Figure 9) and lost 75cm snow depth.
Using the triangle-size, the loss in snow depth and the density of 393,12 kg/m^3 indicates a loss of 294,84mm water equivalent or a water output from the patch of app. 556m^3 through the two weeks (assuming a linear correlation of snowpatch size and snow depth).

‣ Figure 10 shows how the patch is exposed to direct solar radiation. Surrounding landscape covers a large part of the sun progression, resulting in a decreased shortwave radiation energy input. During 5:00 to 14:00 and 22:00 to 24:00, the effective horizon allows approximately 11 of originally 24 hours of direct solar radiation onto the snowpatch. Actually, for 5:00 to 8:00 and 22:00 to 24:00, the sunlight comes in from less than 20° above the horizon and is therefore fairly weak. In Addition, the early morning would be the time with the highest efficiency due to the exposure in east-north-eastern direction. Direct shortwave radiation can therefore not contribute a large amount of energy for melting. However, diffuse solar radiation can still provide energy.

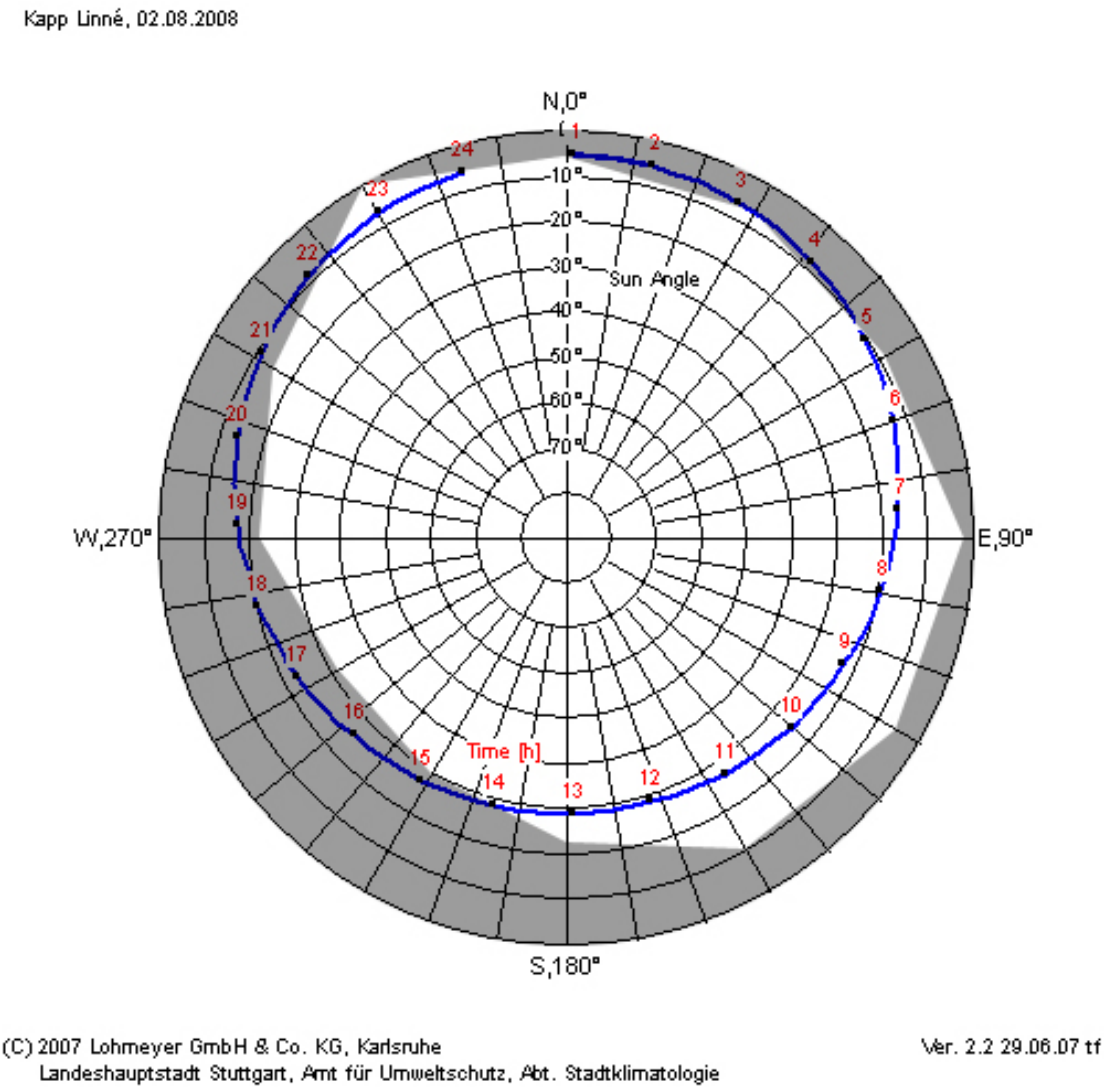

Figure 10: Effective horizon (grey) and progression of the sun (blue line) on the snowpatch on the 2nd of August. Modified according to given source, http://cgi.stadtklima-stuttgart.de/mirror/sonnefre.exe (21.11.2008). Coordinates used for sun progression: 78°01'N, 13°48'E

The 26th of July shows cloudy but bright conditions. The temperature on the slope is relatively high (6,4°C) and the presence of wind (avg. 5,5m/s) can make it available for sensible heat fluxes. The clouds can act as diffuser for the shortwave radiation. This would fit to the cloudy but bright-looking pictures. Together this results in a loss of 182px in size.

The low clouds on the next day seem not to contribute a lot of energy – the value produced with the Plumecam-pictures rises slightly for this day. The amount is insignificant, but it shows that radiation effects not only take place in the energy budget but also in this analysis method. However, the value has to be counted as "no

change", although the snow depth measurement produced the peak loss value for the 26th to the 28th of July. This has to be ascribed to the high ablation rate on the first day.

The peak rate for loss in size arises from the 28th to 29th of July. Again, temperatures are above 6°C on this day. As temperature decreases down to 2,7°C on the next day, the patch decreases only a few pixels in size. This indicates that melt is pretty much temperature driven at this point. Some slight precipitation and even the overcast conditions on the 29th don't arise as a support of longwave radiation in the size and depth data.

On the 1st of August a situation similar to the 26th of July occurs, where clouds increase the shortwave radiation input to the snow surface due to diffusion. On the 30th of July an increased amount of impurities on the snow surfaces was noticed, which reduces albedo and therewith increases the effects of shortwave radiation. Since the measurements of snow depth were only taken every other day and due to a lack of size data because of low clouds on the next day, the precise loss of depth or size is not available. Still, the data table shows that ablation was relatively high for this day.

The overcast conditions from the 2nd to the 4th of August again only contribute little effect to melting. The air with high humidity for these days cannot contribute more than its sensible heat, since the snowpack is isothermal by far and hence the water doesn't freeze onto the snow grains and liberate latent heat.
During the fieldwork, at this point the surface of the inclined snowpatch successively developed horizontal cracks. In addition, some creeping of the snowpack in downslope direction was noticed at the bottom of the snowpatch when doing the transect snow depth measurements along a fixed line. These two observations indicate that gravity forces caused deformations within the snowpack. Mechanical properties of snow are fairly complex. However, snow is a visco-plastic material that starts to creep as soon as a very small threshold stress is applied (Langham, 1981: 299). Therefore, manipulation of the measurements due to snowpack transformation processes cannot be ruled out, especially because the surface showed evidence.
On the 4th / 5th of August this can be the case: The data shows 11,8cm loss in snow depth within 2 days before, where the 4th doesn't show significant melt activity. On the contrary, the size didn't change a lot within this one day. Although high

temperatures would support melting, the shortwave radiation on the 5th cannot contribute a lot of energy and the meltrate is low.

Overcast conditions and slow melting dominate the time from the 5th to the 9th of August. Only the 5th shows clear sky conditions and a higher loss in size from the 5th to the 6th. Although average air temperature is fairly low, the high-resolution raw data provides that temperatures remained high in the afternoon of the 5th.

7 Discussion

7.1 Correlation of SCA and snow depth

The Plumecam-data shows the temporal decline in snow-covered area. In this work, mainly the influences of weather conditions on the SCA are studied. Obviously there is a connection to the decline in water equivalent stored in the catchment as snow, but due to the terrain roughness SCA is not a linear function of water equivalent. Ferguson (1999: 210-212) shows the relationship between spatial variability in snow depth and melt rate and the temporal decline in SCA:

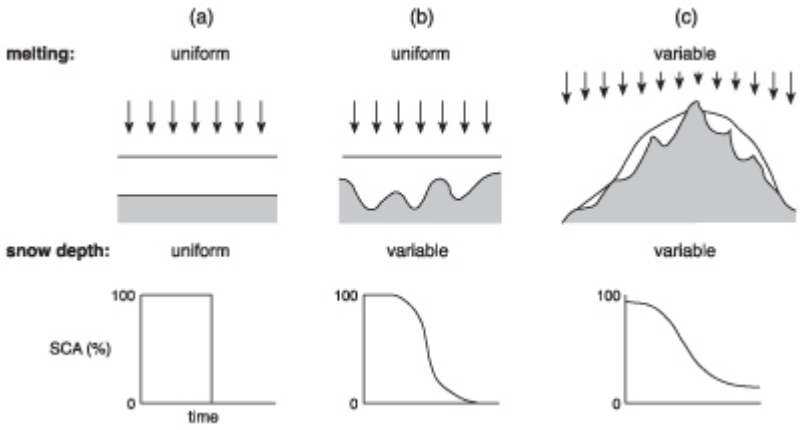

Figure 11: Relation of melt rate, snow depth and SCA. Source: Ferguson (1999: 211)

Linnédalen can be seen as a combination of (b) and (c) and both with a melt rate that is variable under time and location. The figure shows that already a uniform melt rate leads to a non-linear reduction of SCA on every natural terrain. This has to be taken into account, especially when referring to runoff. A fast decline in the SCA-plot doesn't equal a high loss in water equivalent and therefore peak discharge.

However, this figure shows nicely where the s-shape in the SCA-plot originates. As long as the above is taken into account, the data from Linnédalen still offers a nice proxy for analysing the melting period.

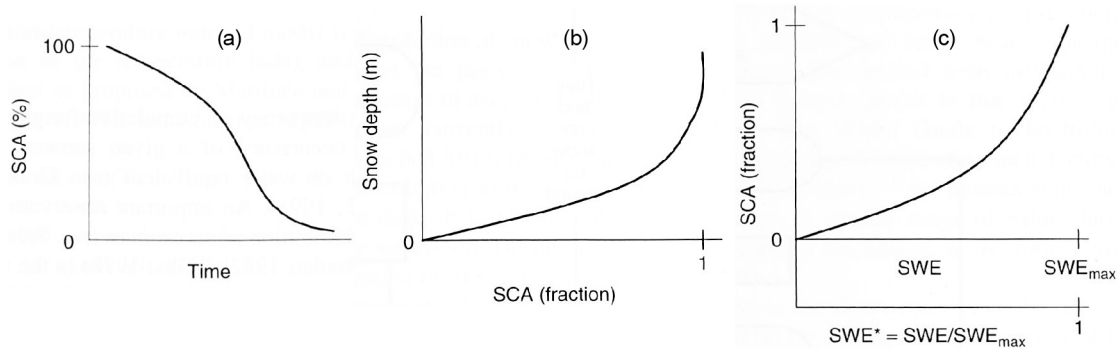

Figure 12: Relation of SCA and time (a), snow depth and SCA (b), SCA and water equivalent (c) (Source: Davison and Pietroniro, 2005: 2516)

Davison and Pietroniro (2005: 2516) show snow depletion curves, which can provide basin-specific information on the temporal decline in SCA. ‣ Figure 12 (a) shows the decrease in SCA, plotted over time. This is what is done in this work and goes in line with the data from Linnédalen. However, this curve is not very meaningful regarding basin-specific properties because it takes the temporal variability of snowmelt into account as it is done in this work. More interesting is the fact that a snowpack tends to follow the same spatial pattern when melting every season (Davison and Pietroniro, 2005: 1516). This means that snow depth decrease and SCA decrease follow a similar correlation every spring. ‣ Figure 12 (b) shows how such a spatial, landcover specific correlation can look like. ‣ Figure 12 (c) is based on the same idea but shows a correlation of water equivalent and SCA.

This terrain specific feature shows up nicely in the SCA data from Linnédalen. As mentioned above, the temporal decline in SCA happens differently on the western and the eastern valley floor. The eastern floor shows a more rapid decrease in SCA, tending a little to Ferguson's (1999: 211) graph in ‣ Figure 11 (a), while the western floor shows an earlier beginning in decrease, which can indicate that the land surface is rougher and has some points that poke out of the snow surface earlier. The latter is represented in Ferguson's (1999: 211) graph (b) or even (c) when neglecting the variable spatial snow distribution.
This means that the area-specific correlation between snow depth and SCA – like it is pointed out by Davison and Pietroniro (2005: 1516) – is different in the two areas.

The correlation curve in ‣ Figure 12 (b) would be bent less for western side and bent more for the eastern side.
Obviously, it could also be differences in the spatial distribution of snow that cause differences in how the melting takes place on the valley floor, but this cannot explain the faster decline in SCA on the eastern floor. However, an overlay of both factors cannot be ruled out, since there is no spatial distributed snow depth data available.

The ideal way of improving the explanatory power of the SCA-data would be to obtain such area-specific information about which SCA equals which snow depth. This would allow making up at least for the non-linear correlation of snow depth and SCA. One idea for this project is to calibrate the SCA-data somehow – so measurements for snow depth were taken among others in the field and are taken into account when analysing the melting period.

7.2 SCA data quality

The data, which was obtained by analysing the plumecam pictures, is assumed to be in some way representative for the whole Linnédalen catchment. This assumption is fairly rude, since the image section only includes parts of the valley floor and the western slope. Especially in the southern part of the valley the topography becomes more complex and Linnébreen acts a part in the hydrological system. Since the image section was fixed, this had to be neglected for the analysis. The contributing conditions in this mesoscale area should be homogenous enough to tolerate this issue, but including other areas in the analysis (like e.g. the eastern slope) would be interesting.

The analysis showed that splitting the image section apart was reasonable. The temporal decrease in SCA on the western slope is not very meaningful. If the raw, aggregated data (no splitting) was used, the slope data had flattened the depletion curve. Furthermore, this technique almost bypassed the problem of perspective bias. The eastern valley floor is still situated in the image foreground, but the data for the different areas isn't accumulated during analysis. Hence, the eastern floor as a whole isn't overweighted. Still, inside the areas, there is some perspective bias, but it shouldn't cause significant failures: Snow-covered and snow-free areas are both weighted higher in the foreground, as they would be in the background. This means, only if the SCA within one of the three areas is heterogeneous, then the SCA in the

foreground in this certain area is weighted higher than in the background. Additionally, the distance to the camera is already fairly large for the eastern valley floor area, which decreases the perspective bias.
The camera's low angle of view causes some bias when the land surface is tilted. A tilt towards the camera lens causes a better exposure and therefore a higher weighting. On the valley floor, this is only the case on small scale, e.g. small ridges, where the face is weighted higher and backside is neglected since it is hidden or at least weighted lower. The slope as a whole has this feature and therefore makes up a separate area in the analysis.

7.3 Data dificulties

Unfortunately, the biggest part of the melting period was already over when the fieldwork started on the 17th of July and the measurements were taken even later. Then, for logistical reasons, the measurements were done only every other day. This results in a total of only eight values each. Difficulties in the analysis of the snowpatch's melting show that especially the two-day-resolution is fairly coarse for analysis on this small scale.
In addition, the accuracy of some results from this time span is questionable. As mentioned in the analysis part, motion of the snowpack may affect the snow depth values. Taking depth measurements not at one spot only but distributed all over the snowpatch or along a stretch could solve this problem. The latter was done in the field by gauging depth twice every meter along a horizontal 16-meter stretch. Processing the data of this transect could have provided reliable data for snow depth, but the stretch of originally 16 meters melted down to 3 meters length. This thwarts the idea of heaving multiple values to average and hence, I don't see a way to integrate this data, so it is neglected.
For a reliable calibration, a representative value for snow depth on the same temporal resolution and for the same period as the pictures would be helpful. Additionally, this value should be representative for the whole camera's field of view. Goodison et al. (1981: 214) suggest to deploy stakes in the area of interest that have a coloured, vertical scale that is large enough to be read remotely – in this case from the camera's pictures. This would be a way of gaining widely distributed snow depth data through the whole season without a lot of effort.

However, the first important progress would be to obtain data from the whole melting period. Especially some additional information about either the liquid water content or water output from the snowpack would help to make out the hydrological periods of melting precisely.
To gain water equivalent values density values are necessary as well, but as long as information about the actually released amount of water (in litres) is unimportant, it is only required to identify SCA-decrease due to compaction of snow. In the runoff phase, were amounts of melted snow are interesting, the pore space holding capacity is reached anyway and density doesn't perform major changes. So, snow depth decrease correlates well with loss in water equivalent in this period.

7.4 Remote sensing of snow

The main advantage of the SCA proxy is the easy way of measuring. The SCA data can be gained from distance, using this early version of "remote sensing". An evaluation of water equivalent requires depth and density measurements that are not as easy to obtain and take a lot of time and work. Additionally, snow depth is extremely variable in the terrain and hence requires extensive gauging.
Remote sensing methods can be used to gain numerous data about the snowpack, including water equivalent. König et al. (2001: 10-12) give an overview about remote sensing of snow and glacier ice. They show that the microwave region allows mapping of water equivalent since it penetrates into the snowpack.
The disadvantage of using satellite data is not only the spatial, but also the temporal resolution, which varies widely from less than a day to several weeks. In addition the optical properties of snow are complex and it is difficult to distinguish between snow and clouds in some bands and between snow and land surface in other bands. The "Plumecam-Method" cannot offer the same sophisticated data, but is easy to use and still provides useful information

8 Attachments

8.1 SCA & weather station data

	SCA				Weather station data			
	Active Area	Slope	Western floor	Eastern floor	Rain (mm)	Windspeed (m/s)	Albedo	Temperature (°C)
17.05.08	99,58%	98,81%	99,74%	100,00%	0	1,40	0,85	-2,01
18.05.08	99,33%	97,96%	99,67%	100,00%	0	2,90	0,85	-2,18
19.05.08	99,27%	97,67%	99,68%	100,00%	0	1,57	0,84	-3,15
20.05.08	98,90%	96,29%	99,62%	100,00%	0	1,33	0,83	-3,14
21.05.08	97,83%	92,78%	99,22%	100,00%	0	4,26	0,81	-2,04
22.05.08	97,21%	90,52%	99,08%	99,99%	0	3,71	0,83	-0,83
23.05.08	97,26%	90,85%	99,01%	100,00%	0,2	3,28	0,81	0,00
24.05.08	98,20%	94,28%	99,22%	100,00%	0	0,78	0,81	-0,67
25.05.08	97,50%	92,04%	98,92%	99,99%	0	1,95	0,78	0,64
26.05.08	97,34%	91,49%	98,87%	99,99%	2	2,71	0,77	0,60
27.05.08	98,10%	93,92%	99,19%	100,00%	0,2	0,79	0,79	0,64
28.05.08	97,52%	92,31%	98,83%	99,99%	0	2,51	0,76	1,14
29.05.08					0	2,45	0,76	-0,04
30.05.08					0	4,98	0,73	1,58
31.05.08					0	4,72	0,69	2,20
01.06.08					0,6	3,09	0,62	2,44
02.06.08					6,6	3,81	0,54	2,04
03.06.08	95,96%	89,02%	97,39%	99,82%	0,2	5,84	0,62	1,07
04.06.08	94,74%	85,06%	96,94%	99,78%	0	0,92	0,72	1,51
05.06.08	92,66%	82,94%	93,81%	99,75%	0	0,89	0,71	1,67
06.06.08	93,60%	82,08%	96,42%	99,18%	0	1,62	0,54	0,17
07.06.08	94,11%	82,74%	96,91%	99,61%	0	0,80	0,53	1,46
08.06.08	91,02%	77,85%	94,67%	96,61%	0	0,98	0,53	1,12
09.06.08	91,69%	79,31%	95,01%	97,16%	0	1,14	0,46	1,63
10.06.08	89,89%	76,13%	93,79%	95,55%	0	2,78	0,42	2,07
11.06.08	90,72%	75,38%	94,72%	97,70%	0,2	4,36	0,38	1,70
12.06.08	87,90%	72,30%	92,38%	94,19%	0	3,36	0,37	1,80
13.06.08	87,86%	72,15%	91,77%	95,35%	0	6,32	0,34	1,58
14.06.08	87,95%	70,11%	92,87%	95,56%	0	4,44	0,33	1,21
15.06.08	84,77%	69,13%	88,50%	92,53%	0	8,19	0,33	0,45
16.06.08	86,03%	67,12%	91,22%	94,12%	0	3,61	0,34	0,74
17.06.08	84,54%	65,73%	89,57%	92,83%	0	2,28	0,32	0,45
18.06.08	83,59%	63,65%	88,87%	92,48%	0	2,93	0,31	0,72
19.06.08	84,28%	65,80%	89,26%	92,38%	0	2,61	0,29	1,53
20.06.08	82,89%	63,35%	88,22%	91,31%	0	2,02	0,29	1,56
21.06.08	82,76%	63,55%	88,09%	90,87%	0	0,84	0,36	3,38
22.06.08					13,2	3,48	0,20	3,01
23.06.08	76,53%	59,56%	81,34%	83,50%	1,8	4,41	0,20	3,03
24.06.08	72,40%	57,30%	77,23%	77,54%	0,4	2,23	0,20	2,81
25.06.08	70,94%	58,25%	76,02%	73,30%	0,2	2,10	0,20	3,56
26.06.08	65,42%	53,72%	69,89%	67,99%	0	4,32	0,20	5,43
27.06.08	54,34%	50,38%	59,40%	48,41%	0	3,84	0,20	6,06
28.06.08	56,79%	53,57%	63,40%	47,15%	0	4,59	0,17	4,60
29.06.08	49,47%	51,92%	54,79%	36,88%	0	3,49	0,18	5,47
30.06.08	48,08%	52,98%	52,99%	33,95%	5	2,84	0,17	5,13

01.07.08	44,43%	54,67%	48,14%	27,51%	0,2	2,03	0,14	3,99
02.07.08	44,57%	49,84%	48,66%	31,67%	0	2,92	0,15	4,08
03.07.08	38,22%	47,91%	40,55%	24,49%	0,4	2,51	0,15	3,91
04.07.08					0	2,40	0,17	3,71
05.07.08					0	1,65	0,17	4,52
06.07.08	28,35%	43,33%	28,34%	14,03%	0	3,56	0,19	4,92
07.07.08	30,94%	48,69%	29,22%	17,27%	0	2,63	0,17	5,47
08.07.08	23,09%	42,09%	21,69%	7,61%	0	2,15	0,16	4,14
09.07.08					0,4	6,91	0,15	4,58
10.07.08	23,82%	45,12%	22,32%	6,33%	0	10,22	0,17	2,72
11.07.08					2,2	6,77	0,16	2,25
12.07.08					22,4	3,42	0,10	3,14
13.07.08	17,72%	37,48%	13,42%	7,08%	14,4	5,80	0,13	5,46
14.07.08	18,14%	36,03%	14,74%	7,59%	0	3,26	0,15	6,06
15.07.08	13,87%	31,87%	11,50%	1,22%	0	1,54	0,17	5,63
16.07.08	12,66%	29,68%	10,47%	0,58%	0	1,62	0,22	8,23
17.07.08	12,64%	30,07%	9,92%	1,20%	0	3,04	0,19	8,03
18.07.08	14,35%	30,10%	10,67%	6,36%	0	4,36	0,17	8,36
19.07.08					0,8	2,05	0,15	5,66
20.07.08	10,87%	26,05%	7,84%	2,16%	5,2	3,01	0,15	6,02
21.07.08					1	2,42	0,14	6,51
22.07.08	9,65%	24,03%	6,12%	2,69%	0	2,71	0,18	8,92
23.07.08	9,34%	23,10%	7,04%	0,60%	0	3,80	0,21	10,15
24.07.08	8,98%	22,81%	6,31%	0,90%	0	3,09	0,21	6,54
25.07.08	8,46%	21,49%	5,31%	2,06%	0	1,94	0,17	7,35
26.07.08	10,58%	26,36%	5,43%	5,38%	0	5,46	0,17	7,12
27.07.08					0	3,14	0,17	5,85
28.07.08	8,60%	20,27%	5,78%	2,87%	0	2,69	0,18	5,93
29.07.08	7,07%	20,42%	3,76%	0,66%	0,4	5,16	0,15	4,84
30.07.08	6,61%	16,38%	4,23%	1,83%	0	3,34	0,18	4,59
31.07.08	6,43%	16,60%	3,77%	1,83%	0	2,29	0,19	6,72
01.08.08					0	3,63	0,19	5,32
02.08.08					0	1,71	0,17	3,77
03.08.08					0	1,70	0,17	3,55
04.08.08					0	2,35	0,18	5,17
05.08.08	6,05%	15,01%	4,01%	1,40%	0	4,68	0,19	5,66
06.08.08	5,10%	13,24%	2,50%	2,33%	0	6,80	0,18	3,75
07.08.08	4,93%	13,01%	2,35%	2,18%	0	4,88	0,19	4,55
08.08.08	3,81%	10,83%	2,18%	0,21%	0,6	3,23	0,16	4,40
09.08.08	4,36%	12,70%	2,22%	0,50%	2,4	2,25	0,14	3,78
10.08.08	3,71%	11,30%	1,63%	0,44%	2	1,27	0,15	3,20
11.08.08	5,01%	12,45%	2,06%	3,59%	4,6	2,31	0,13	4,24

Attachment 1: SCA and weather station data table

8.2 Western slope data

		Measured		LIA moraine logger		Main weather station	
	Size (pixel)	Size (m^2)	Snow depth (cm)	Temperature (°C)	Humidity (%)	Rain (mm)	Wind (m/s)
26.07.08	2362,00	2298,80	212,40			0	5,46
27.07.08	2180,00			6,40	82,24	0	3,14
28.07.08	2214,00	2065,55	195,00	4,03	93,30	0	2,69
29.07.08	1998,00			6,23	89,19	0,4	5,16
30.07.08	1994,00	1411,83	180,80	2,74	85,97	0	3,34
31.07.08	1981,00			4,40	76,71	0	2,29
01.08.08		1419,60	173,20	7,49	69,33	0	3,63
02.08.08	1772,00			3,22	95,77	0	1,71
03.08.08		1398,02	165,80	3,33	96,96	0	1,70
04.08.08	1687,00			2,83	98,35	0	2,35
05.08.08	1667,00	1312,16	154,00	6,26	81,80	0	4,68
06.08.08	1576,00			3,88	78,93	0	6,80
07.08.08	1556,00	1276,76	144,80	3,20	81,94	0	4,88
08.08.08	1528,00			3,77	71,13	0,6	3,23
09.08.08	1502,00	1242,78	137,60	3,96	86,57	2,4	2,25

Attachment 2: Snowpatch measurements and weather conditions overview table

8.3 Snowtree data

	Temperature (°C)		
	7cm above ground	15cm above ground	30cm above ground
01.05.08	-0,55	-1,00	-1,34
02.05.08	-0,55	-1,00	-1,34
03.05.08	-0,55	-1,00	-1,34
04.05.08	-0,56	-1,00	-1,34
05.05.08	-0,56	-0,99	-1,34
06.05.08	-0,56	-0,98	-1,34
07.05.08	-0,56	-0,97	-1,34
08.05.08	-0,56	-0,95	-1,34
09.05.08	-0,55	-0,90	-1,30
10.05.08	-0,55	-0,89	-1,23
11.05.08	-0,55	-0,89	-1,23
12.05.08	-0,55	-0,89	-1,23
13.05.08	-0,55	-0,89	-1,23
14.05.08	-0,55	-0,89	-1,23
15.05.08	-0,55	-0,89	-1,22
16.05.08	-0,55	-0,89	-1,15
17.05.08	-0,55	-0,89	-1,11
18.05.08	-0,55	-0,88	-1,11
19.05.08	-0,55	-0,84	-1,11
20.05.08	-0,55	-0,78	-1,09
21.05.08	-0,55	-0,77	-1,00
22.05.08	-0,55	-0,77	-1,00
23.05.08	-0,55	-0,77	-1,00
24.05.08	-0,55	-0,77	-0,96
25.05.08	-0,55	-0,77	-0,89
26.05.08	-0,51	-0,70	-0,89
27.05.08	-0,23	-0,59	-0,81
28.05.08	-0,21	-0,49	-0,71
29.05.08	-0,21	-0,44	-0,65
30.05.08	-0,21	-0,43	-0,56
31.05.08	-0,10	-0,28	-0,34
01.06.08	-0,10	-0,12	-0,10
02.06.08	-0,10	-0,10	-0,10
03.06.08	-0,10	-0,10	-0,10

Attachment 3: Snowtree data table

8.4 Snowpatch snow depth – stretch method

Distance	24.07.08	26.07.08	28.07.08	30.07.08	01.08.08	03.08.08	05.08.08	07.08.08	09.08.08
0	42,5	0	0	0	0	0	0	0	0
1	52,5	37,5	20,5	3,5	0	0	0	0	0
2	65	45	27	23,5	8,5	10,5	0	0	0
3	74	50	42,5	32	21	16,5	0	0	0
4	71	60	55	32,5	24	10	0	0	0
5	74	65	42,5	27,5	30	32	0	0	0
6	76,5	75	57,5	29	24,5	21	0	0	0
7	75	66	37,5	32,5	20,5	10	0	0	0
8	77,5	57,5	45	32	25	21	5	2,5	0
9	85	65	57,5	43,5	35	33,5	21	2,5	0
10	112,5	71	62,5	51,5	41	35	20	11,5	10
11	115	78,5	65	51,5	46,5	36,5	33,5	25,5	21,5
12	87,5	96,5	86	61,5	45,5	51	32	30	17
13	97,5	90	69	56,5	45	35	22,5	25	0
14	77,5	77,5	57	57,5	42,5	35,5	24	15	8
15	42,5	55	40	38,5	27,5	0	0	0	0
16	20	35	0	0	0	0	0	0	0

Attachment 4: Snowpatch snow depth; stretch method

8.5 SCA plotted over time

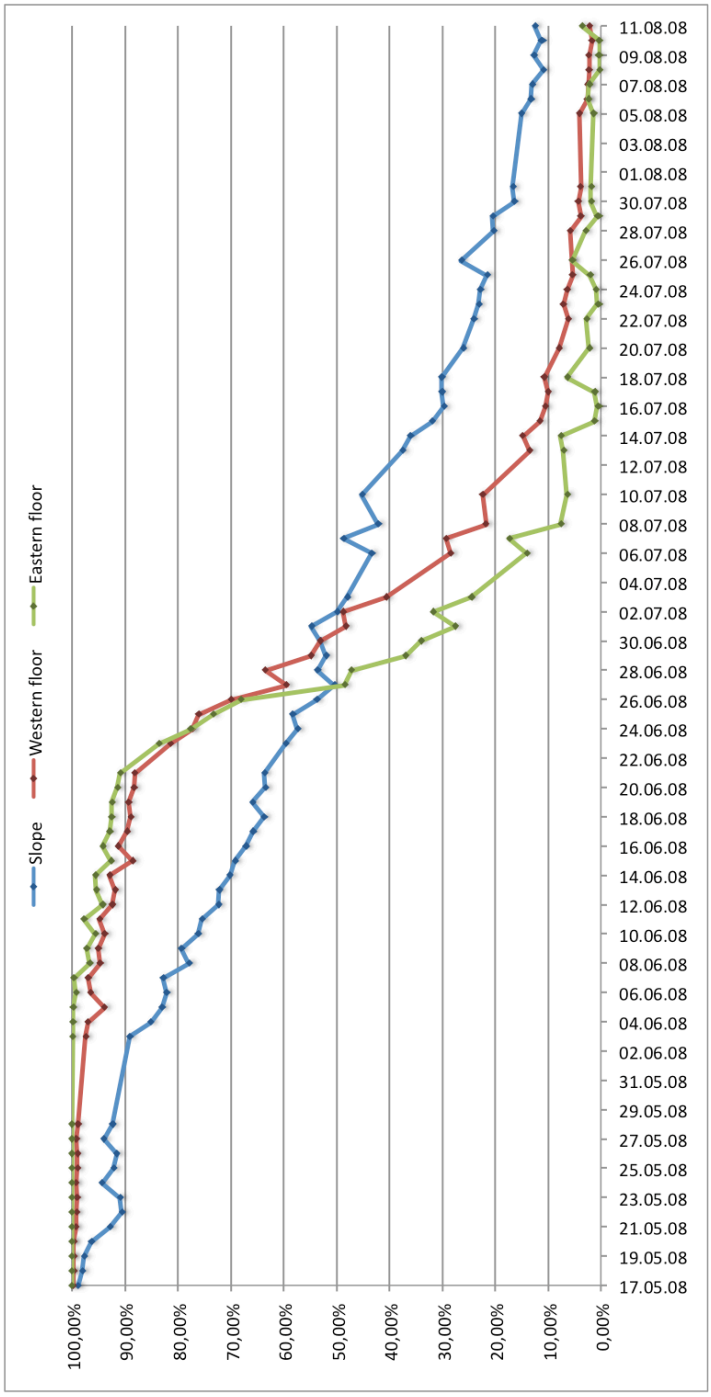

Attachment 5: SCA of slope, western and eastern valley floor plotted over time

8.6 Topographic map

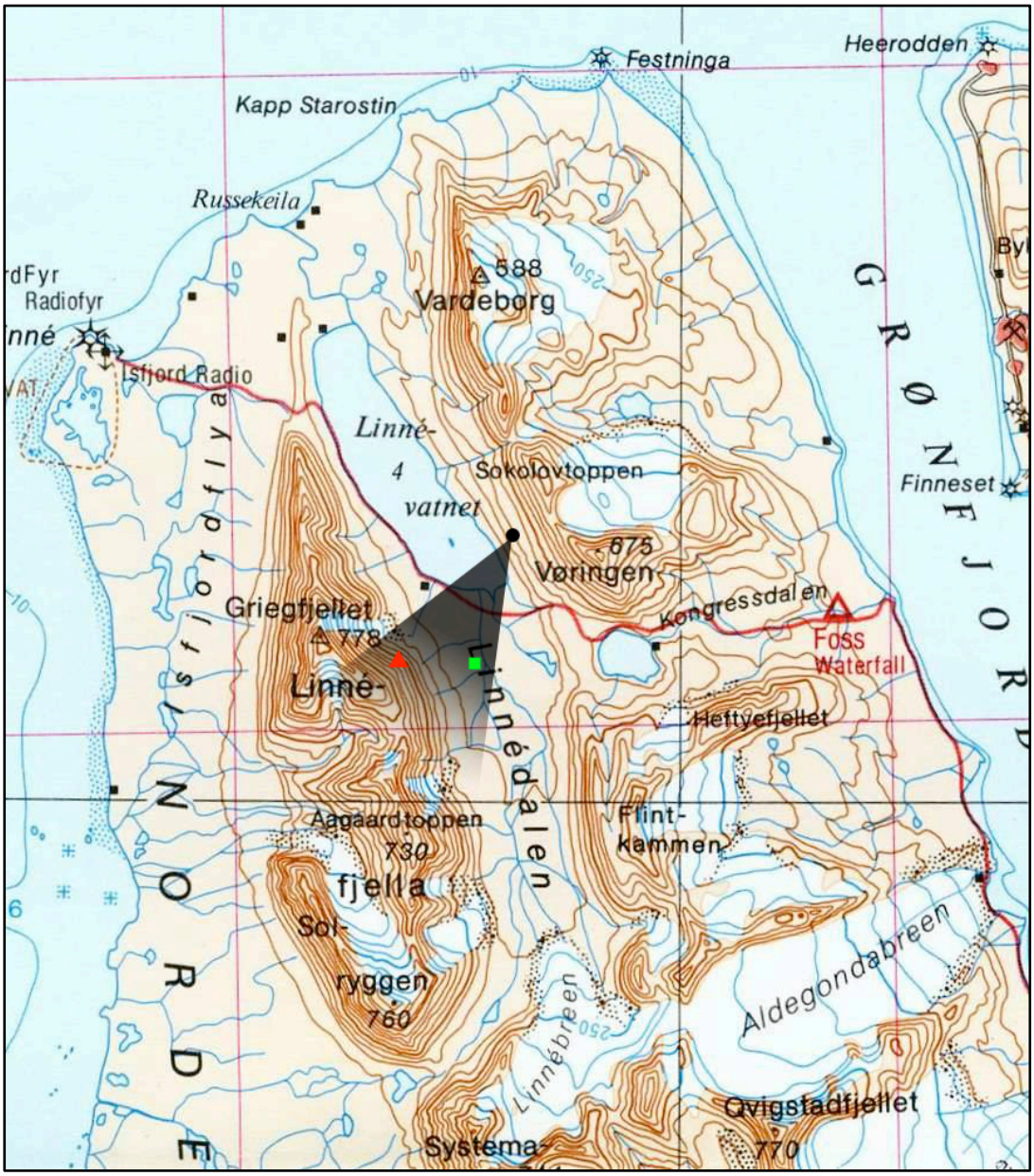

Attachment 6: Modified section of topographic map of Linnédalen. False scale due to scan, resize and print.
Copyright: Norsk Polarinstitutt
Black: Plumecam position and angle of view
Red triangle: snowpatch position
Green square: approximate weather station position

9 Literature

American Avalanche Association. 2004: Snow, Weather and Avalanches: Observational Guidelines for Avalanche Programs in the United States. USDA Forest Service National Avalanche Center, Pagosa Springs. 136 pp.

Anisimov, O.A., D.G. Vaughan, T.V. Callaghan, C. Furgal, H. Marchant, T.D. Prowse, H. Vilhja´lmsson, J.E. Walsh. 2007: Polar regions (Arctic and Antarctic). *Climate Change 2007: Impacts, Adaptation and Vulnerability. Contribution of Working Group II to the Fourth Assessment Report of the Intergovernmental Panel on Climate Change*. Cambridge University Press, Cambridge, 653-685.

Davison, B., A. Pietroniro. 2005: Hydrology of Snowcovered Basins. *Encyclopedia of Hydrological Sciences*, M.G. Anderson (ed.). John Wiley & Sons, Chichester, 2505-2532.

Dingman, S.L. 2002: Physical Hydrology. Prentice-Hall, New Jersey. 646 pp.

Gerland, S., J-G. Winther, J.B. Ørbæk, G.E. Liston, N.A. Øritsland, A. Blanco, B. Ivanov. 1999: Physical and optical properties of snow covering Arctic tundra on Svalbard. *Hydrological Processes* **13** (14-15), 2331-2343.

Goodison, E.J., H.L. Ferguson, G.A. McKay. 1981: Measurements and Data Analysis. *Handbook of snow*, D.M. Gray, D.H. Male (eds.). Pergamon Press, Toronto, 191-274.

Gray, D.M., D.H. Male. 1981: Snowcover Ablation and Runoff. *Handbook of snow*, D.M. Gray, D.H. Male (eds.). Pergamon Press, Toronto, 360-436.

Gray, D.M., T. Prowse. 1993: Snow and Floating Ice. *Handbook of Hydrology*, D.R. Maidment (ed.). Mcgraw-Hill Professional, New York. 1424 pp.

Hock, R. 2005: Glacier melt: a review of processes and their modelling. *Progress in Physical Geography* **29** (3), 362–391.

King, J.C., J.W. Pomeroy, D.M. Gray, C. Fierz, P.M.B. Föhn, R.J. Harding, R.E. Jordan, E. Martin, C. Plüss. 2008: Snow-atmosphere energy and mass balance. *Snow and Climate: Physical Processes, Surface Energy Exchange and Modeling*, Armstrong, R.L., E. Brun (eds.). Cambridge University Press, Cambridge, 70-124.

König, M., J-G. Winther, E. Isaksson. 2001: Measuring Snow and Glacier Ice Properties from Satellite. *Reviews of Geophysics* **39** (1), 1-27.

Landeshauptstadt Stuttgart, Amt für Umweltschutz, Abt. Stadtklimatologie. 2007: Sun's location / Sonnenstand. *http://cgi.stadtklima-stuttgart.de/mirror/sonnefre.exe* (21.11.2007).

Langham, E.J. 1981: Physics and Properties of Snowcover. *Handbook of snow*, D.M. Gray, D.H. Male (eds.). Pergamon Press, Toronto, 275-337.

Liston, G.E. 1995: Local Advection of Momentum, Heat and Moisture during the Melt of Patchy Snow Covers. *Journal of Applied Meteorology* **34**, 1705-1715.

Marsh, P. 1999: Snowcover formation and melt: recent advances and future prospects. *Hydrological Processes* **13** (14-15), 2117-2134.

Pohl, S., P. Marsh. 2006: Modelling the spatial-temporal variability of spring snowmelt in an arctic catchment. *Hydrological Processes* **20** (8), 1773 – 1792.

Winther, J-G., S. Gerland, J.B. Ørbæk, B. Ivanov, A. Blanco, J. Boike. 1999: Spectral reflectance of melting snow in a high Arctic watershed on Svalbard: some implications for optical satellite remote sensing studies. *Hydrological Processes* **13** (12-13), 2033-2049.

Zhang, T., K. Stamnes, S.A. Bowling. 1996: Impact of Clouds on Surface Radiative Fluxes and Snowmelt in the Arctic and Subarctic. *Journal of Climate* **9**(9), 2110–2123.